PNAS

Supporting Information for

The mRNA Translation Initiation Factor eIF4G1 Controls Mitochondrial Oxidative Phosphorylation, Axonal Morphogenesis, and Memory

Sung-Hoon Kim, Jung-Hyun Choi, Laura Marsal-García, Mehdi Amiri, Akiko Yanagiya, and Nahum Sonenberg*

*Correspondence: Dr. Nahum Sonenberg (nahum.sonenberg@mcgill.ca)

This PDF file includes:

Supporting Text

Comparison of eIF4E and eIF4G1 in cognitive function

Eukaryotic initiation factor 4F (eIF4F) consists of the cap-binding protein eIF4E, ATP-dependent RNA helicase eIF4A (eIF4A1), and scaffolding protein eIF4G (eIF4G1). eIF4E and eIF4G1 are involved in eukaryotic cap-dependent translation, and eIF4G1 is required for the canonical internal ribosome entry site (IRES)-mediated cap-independent translation (1). Translation of mRNAs with highly structured 5'-UTR is sensitive to eIF4E (2), whereas the translation of mRNAs with long 3'-UTR, multiple upstream open reading frames (uORFs), or TISU in 5'-UTR is sensitive to eIF4G1 (3, 4). Both proteins are indispensable for early development since homozygous CRISPR-Cas9 knockout of either gene displayed embryonic lethality in mice (5). Nonetheless, partial silencing of either protein does not significantly affect global translation (3, 6).

Inhibition of the interaction between eIF4E and eIF4G1 by 4EGI-1 disrupts long-term memory consolidation (7), demonstrating that the interaction is critical for cognition. Many previous studies that manipulated the molecular abundance or activity of the proteins have shown the contributions of eIF4E and eIF4G1 to cognition and brain disorders, as summarized in Table S1.

Cell-type-specific eIF4E knockdown in specific brain regions displays impairment in long-term emotional memory (8, 9), while eIF4E transgenic mice show ASD-like behaviors (10). eIF4E activity is suppressed by eIF4E-binding proteins 4E-BPs. 4E-BP2 knockout mice similarly manifest ASD-like behaviors (11), and 4E-BP2 conditional knockout mice exhibit cell-type-specific behavioral alterations, such as spatial memory and motor impairment or increased pentylenetetrazole (PTZ)-induced seizures (12, 13). eIF4E S209A knockin mice harboring non-phosphorylatable eIF4E show depression and anxiety-like behaviors (14, 15).

In contrast to eIF4E, little is known about the role of eIF4G1 in cognition. Elevation of eIF4G1 in the brain by decreased CUL3, E3 ubiquitin ligase of eIF4G1, exhibits social deficits and anxiety-like behaviors (16). Disruption of microexon in eIF4G1 leads to learning and memory deficits and autistic-like behaviors (17); however, the mechanism by which downregulation of eIF4G1 levels affects mouse behaviors remains unknown.

SI Materials and Methods

Immunofluorescence (IF)

Cells seeded on the poly-D-lysine (Sigma)-coated coverslip were fixed by pre-cooled 4% PFA (Electron Microscopy Sciences) for 15 min on ice. After being washed 3 times by PBS, cells were permeabilized by PBS containing 0.1% Triton X-100 (Thermo Fisher Scientific) for 15 min on ice and blocked by PBS containing 2% BSA for 1 hr at room temperature. Cells were incubated with primary antibodies overnight at 4℃ and incubated with Alexa Fluor-conjugated secondary antibodies (Thermo Fisher Scientific) for 1 hr at room temperature in the darkness. Cover glasses were mounted onto the slide glass by using the ProLong Diamond Antifade Mountant with DAPI (Thermo Fisher Scientific).

Subcellular Fractionation

Subcellular fractionation was performed as previously described (18). Briefly, a whole mouse brain was homogenized in homogenization buffer (4 mM HEPES pH 7.4, 1 mM EGTA, 320 mM sucrose, 1 mM PMSF) in a pre-chilled Dounce homogenizer on ice. The homogenate was centrifuged at 1,000 x g for 10 min at 4℃. The nuclear and debris pellet (P1) was saved, and the post-nuclear supernatant (S1) was centrifuged at 9,200 x g for 15 min at 4℃. The crude cytosol supernatant (S2) was saved, and the crude synaptosomal pellet (P2) was washed twice by homogenization buffer and centrifuged at 10,200 x g for 15 min at 4℃. The washed P2 was lysed by osmotic shock with ice-cold distilled water, followed by homogenization and centrifugation at 25,000 x g for 20 min at 4℃ to yield the crude synaptic cytosol (SC) and the synaptosomal membrane pellet (P3). The P3 was resuspended in the homogenization buffer and loaded onto a discontinuous sucrose gradient (0.8 M and 1.2 M sucrose). The gradient was centrifuged at 150,000 x g for 1 hr at 4℃. The pellet at the interface region was collected and centrifuged again at 150,000 x g for 30 min at 4℃. The resulting pellet was incubated with ice-cold 0.5% Triton X-100 for 15 min and centrifuged at 32,000 x g for 20 min at 4℃. The Triton X-100-insoluble fraction was collected for the postsynaptic density (PSD), and the supernatant was saved for the extrasynaptic membrane (ESM).

Polysome Profiling

Polysome profiling was performed as previously described (19) with minor modifications. Briefly, a forebrain was dissected from a deeply anesthetized mouse on postnatal day 14 (P14) and immediately frozen with liquid

nitrogen. The frozen brain was homogenized in prechilled hypotonic buffer (5 mM Tris-HCl pH 7.4, 1.5 mM KCl, 2.5 mM $MgCl_2$, 200 µg/ml of cycloheximide (CHX), 300 µg/ml of chloramphenicol (CHL), 200 u/ml of RNase inhibitor, 2 mM DTT, supplemented with EDTA-free protease inhibitor tablet) on ice. The homogenate was lysed by adding a detergent mixture (0.5% of Triton X-100 and 0.5% of sodium deoxycholate) followed by a 5-sec vortex. After being incubated on ice for 5 min, the lysate was centrifuged at 21,130 x g for 5 min at 4℃. The optical density of RNA in the supernatant was measured using NanoDrop 2000 (Thermo Fisher Scientific), and an equal amount of each sample was loaded onto a 10-50% continuous sucrose gradient containing 20 mM HEPES-KOH pH 7.6, 100 mM KCl, 5 mM $MgCl_2$, 20 µg/ml of CHX, 30 µg/ml of CHL, 10 u/ml RNase inhibitor, supplemented with EDTA-free protease inhibitor tablet. Gradients were centrifuged at 36,000 rpm for 2 hr at 4℃ using SW 40 Ti rotor in Optima L-80 XP ultracentrifuge (Beckman Coulter). Absorbance at 254 nm was measured using TracerDAQ (MicroDAQ) from lower to higher sedimentation of sucrose gradients.

RT-qPCR

Total RNA from each polysome fraction was extracted by using Trizol (Invitrogen) according to the manufacturer's instructions. The same volume of RNA, no more than 5 µg from each polysome fraction, was reverse transcribed using oligo(dT)18 and SuperScript III (Invitrogen). The amount of mRNA was analyzed by CFX Connect Real-Time PCR Detection System (Bio-Rad) using SensiFAST SYBR No-ROX Kit (Bioline) and the gene-specific primers. A comparative Ct method was used for quantification.

Library Preparation and Analysis of RNA-Seq and Ribo-Seq

Library preparation for RNA-Seq and Ribo-Seq was performed as previously described (20, 21). Demultiplexing and trimming adapter sequences (AGATCGGAAGAGCACACGTCTGAA) were performed using Cutadapt (22). Shorter than 30 nucleotides or untrimmed RNA-Seq reads were discarded. Likewise, Ribo-Seq reads shorter than 30 nucleotides or longer than 60 nucleotides were discarded. Ribosomal and transfer RNAs were removed using bowtie2's local alignment mode (23). UMI sequences were extracted using UMI-tools (24). The remaining reads were mapped to the mouse genome (UCSC GRCm38/mm10) using HISAT2 (25). PCR duplicates were removed using UMI-tools. Uniquely mapped reads were counted using featureCounts (26). Differential expression analysis was carried out by Z-score analysis as previously described (27), and metagene analysis was carried out with ribosomeProfilingQC R package (28).

Mitochondrial Fluorescent Noncanonical Amino Acid Tagging

Mitochondria-specific fluorescent noncanonical amino acid tagging (mito-FUNCAT) was performed as previously described (29, 30) with minor modifications. Briefly, cells were washed with pre-warmed PBS twice and incubated with methionine-free medium (Dulbecco's Modified Eagle Medium (DMEM) w/o L-Gln, L-Met, L-Cys (Wisent) supplemented with 10% dialyzed FBS (Gibco) and 1% streptomycin-penicillin (Wisent)) containing 50 μg/ml of CHX for 20 min. 500 μM of L-homopropargylglycine (HPG) (Jena Bioscience) was added to the medium for 30 min. Cells were incubated in buffer A (10 mM HEPES, 10 mM NaCl, 5 mM KCl, 300 mM sucrose, 0.015% digitonin) for 2 min on ice, followed by incubated in buffer A without digitonin for 15 sec. Cells were fixed using 4% PFA in PBS for 30 min at room temperature. After being washed with PBS for 5 min, cells were quenched with 100 mM NH_4Cl in PBS for 15 min and permeabilized using 0.1% Triton X-100 in PBS for 10 min. Cells were briefly washed with 2% BSA in PBS, and a copper-catalyzed azide-alkyne cycloaddition (CuAAC) reaction was carried out using Click-iT Cell Reaction Buffer Kit (Invitrogen) with Alexa Flour 488 azide (Invitrogen) according to the manufacturer's instructions. Cells were briefly washed with 2% BSA in PBS and subjected to IF procedure as described above.

Seahorse Glycolysis and Mito Stress Test

Glycolytic capacity and mitochondrial respiration were measured using the Seahorse XFe96 Extracellular Flux Analyzer (Agilent). For measuring mitochondrial respiration, Neuro2A cells were seeded into Polyethyleneimine (PEI) (Sigma) pre-coated Seahorse XFe96 plate (Agilent). On the next day, the culture medium was replaced with Seahorse assay medium supplemented with 10 mM glucose (Agilent), 1 mM sodium pyruvate (Agilent), and 2 mM glutamine (Wisent), pH 7.4, and cells were equilibrated in CO_2-free 37℃ incubator for 1 hr. 1 μM oligomycin (Cayman Chemical), 1 μM carbonyl cyanide-p-trifluoromethoxyphenylhydrazone (FCCP) (Cayman Chemical), 0.5 μM rotenone (Calbiochem), and 0.5 μM antimycin A (Cayman Chemical) were treated as mitochondrial respiratory chain inhibitors, and oxygen consumption rate (OCR) was measured. For measuring glycolytic capacity, Neuro2A cells were prepared as described above. The culture medium was replaced with Seahorse assay medium supplemented with 2 mM glutamine, pH 7.4, and cells were equilibrated in CO_2-free 37℃ incubator for 1 hr. 10 mM glucose, 1 μM oligomycin, and 50 mM 2-deoxy-d-glucose (2-DG) (Sigma) were treated, and extracellular acidification rate (ECAR) was measured.

Monitoring ATP Levels in Living Cells

MaLionR and MaLionG were a gift from Tetsuya Kitaguchi (Addgene plasmid #113908 and #113906, respectively), and MitoMaLionG was made by fusing mitochondrial targeting sequence human cytochrome c oxidase subunit 8A (hCOX8A) to the N-terminus of MaLionG as previously described (31). MaLionR and MitoMaLionG were co-transfected into cells using Lipofectamine 2000 (Invitrogen) according to the manufacturer's instructions. 24 hr after transfection, cells were briefly washed with pre-warmed 1x Hank's Balanced Salt Solution (HBSS) (Gibco) and subjected to confocal imaging.

Measuring Mitochondrial membrane potential ($\Delta\Psi_m$)

$\Delta\Psi_m$ was measured using TMRE-Mitochondrial Membrane Potential Assay Kit (Abcam) according to the manufacturer's instructions. Hoechst 33342 (Invitrogen) or NeuroFlour NeuO (Stemcell Technologies) were co-treated for cell lines or primary neurons, respectively.

Primary Hippocampal Neuron Culture

Hippocampi from E17.5 mouse embryos obtained from eIF4G1 wt x 1D breeding were dissected on ice. The dissected tissues were immediately put into ice-cold Hibernate-E media (Gibco) supplemented with 1x B-27 supplement (Gibco) and stored at 4℃. In the meantime, genomic DNA isolation from a tail of the embryo and genotyping PCR were performed. Hippocampi of the same genotype were pooled together and briefly washed with ice-cold 1x HBSS containing Ca^{2+} and Mg^{2+} (Gibco), followed by ice-cold 1x HBSS without Ca^{2+} and Mg^{2+} (Gibco) twice. Then, the tissues were incubated in pre-warmed trypsin (Gibco) at 37℃ for 13 min with occasional flipping. The solution was replaced with pre-warmed FBS to neutralize the trypsin, and the tissues were washed with pre-warmed trituration media (DMEM supplemented with 10% FBS) twice. Hippocampal neurons were dissociated in 1 ml of trituration media by mild pipetting. Clumps were removed using Cell Strainer (Falcon). Neurons were seeded into plates pre-coated overnight with PEI. After 2 hr, the trituration media were replaced with pre-warmed maintaining media (Neurobasal media (Gibco) supplemented with 1x B-27 supplement, 0.25x GlutaMAX supplement (Gibco), and 1% streptomycin-penicillin). A mixture of 10 μM uridine (Sigma) and 10 μM 5-Fluoro-2'-deoxyuridine (Sigma) was added to the media at DIV2 as a mitotic inhibitor. Fresh media were added every 5 days.

Behavior Tests

Male mice aged 3- to 4-month-old were handled for three consecutive days and habituated to the behavioral room for 30 min prior to the tests. All the tests were conducted in an isolated and soundproof room, and all behavioral apparatuses were cleaned between mice.

Morris Water Maze Morris water maze test was performed as previously described (32). Mice were individually placed in a circular plastic pool (100 cm diameter) filled with water (22±1℃) mixed with nontoxic white paint. On the first day, mice were examined to find a visible platform marked with a distinct flag in four different starting positions and four different platform locations. Mice were gently guided to the platform by the experimenter and remained to stay for 20 sec when they failed to find the platform within 60 sec. During the memory acquisition phases, mice were trained four times per day by being allowed to search for the hidden platform for 60 sec for five consecutive days. On the probe test days, mice were allowed to swim for 60 sec while the platform was removed. Mice were dried for normothermia before being returned to the home cage between every session. The trajectory of mice was recorded using a video tracking system, and the latency to reach the platform, total time spent in each of the four quadrants, and the number of platform crossings was analyzed.

Contextual Fear Conditioning On the training day, two foot-shocks (0.7 mA, 1 sec) separated by 60 sec were administered for 4 min after 2 min of context exploration. 24 hr later, mice were tested in the same context for 5 min. Contextual fear memory was assessed by the percentage of total time spent freezing. The total time spent freezing was manually measured, and the percent of freezing was calculated by a total 5 min period. FreezeFrame was used to carry out the test, and FreezeView to visualize the behavioral videos.

Self-Grooming Test Mice were individually placed in a new home cage containing bedding material but no nesting material and allowed to explore freely for 20 min. The first 10 min was considered to be the habituation phase, and the final 10 min was used to analyze self-grooming behavior. The total time spent grooming and the total number of grooming bouts were manually measured.

Open Field Test Mice were individually placed in a white Plexiglas chamber (40 cm x 40 cm x 40 cm) and allowed to explore freely for 20 min. Total travel distance and total time spent in the center were measured.

Elevated Plus Maze The testing apparatus consists of two closed arms protected by black walls and two open arms with open edges that are 60 cm above the floor, meeting at a center zone to form a plus shape. Mice were individually placed in one of the closed arms and allowed to explore freely for 5 min. The total number of entries and average time spent in the open arms were measured.

Light-Dark Transition Test Mice were individually placed in the light side of the test apparatus, which is composed of two adjacent chambers – a black Plexiglas chamber (20 cm x 40 cm x 40 cm) and a white Plexiglas chamber (20 cm x 40 cm x 40 cm) connected by a small opening. Mice were allowed to explore freely for 10 min, and the total number of entries and average time spent in the light chamber were measured.

Rotarod Mice were introduced to an accelerating rotarod (4 to 40 rpm within 5 min), and the latency to fall for each of the mice was measured unless they fell within 10 sec.

Figure S1. eIF4G1 Protein in the Mouse Brain and Neurons

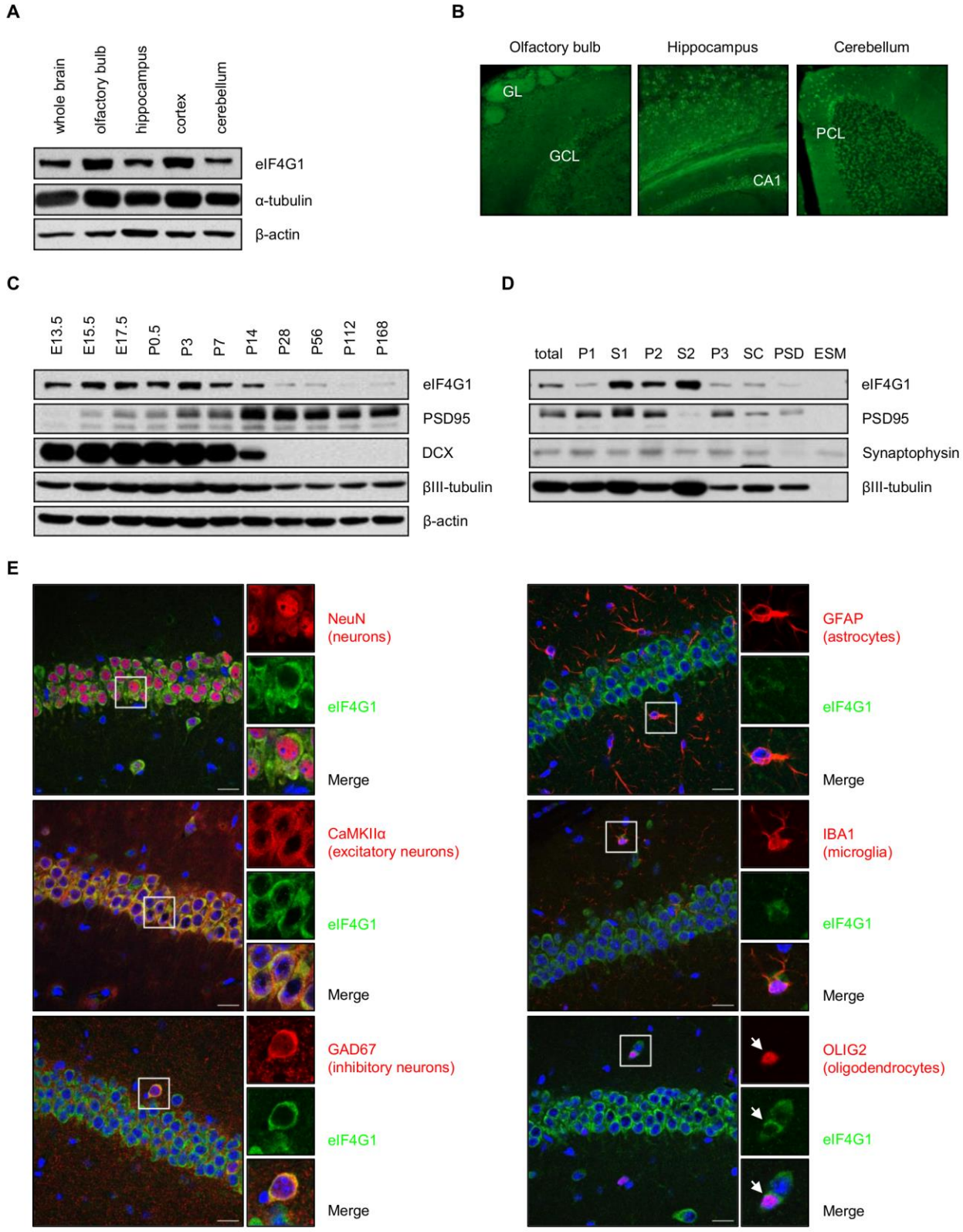

Figure S1. eIF4G1 protein in the mouse brain and neurons

(A) eIF4G1 protein in the mouse brain. Olfactory bulbs, hippocampus, cortex, and cerebellum were dissected from the whole mouse brain and subjected to immunoblot analysis. The eIF4G1 blot was obtained by longer exposure. α-tubulin and β-actin were used as loading controls.

(B) eIF4G1 protein in the mouse brain. eIF4G1 protein (green) was stained in the sagittal section of the eIF4G1 wt brain, and images were focused on the indicated brain area. GL, glomerular layer; GCL, granule cell layer; CA1, cornu amonis 1; PCL, Purkinje cell layer

(C) eIF4G1 protein levels in the developing mouse brain. The whole mouse brain was dissected at the indicated time point and subjected to immunoblot analysis. E and P indicate embryonic and postnatal days, respectively. PSD95 and doublecortin (DCX) were used as control proteins increasing or decreasing during brain development, respectively. βIII-tubulin and β-actin are shown as loading controls.

(D) Subcellular localization of eIF4G1. A whole adult mouse brain was dissected and subjected to a subcellular fractionation assay. PSD95 and synaptophysin were used as control proteins localized in postsynaptic density and presynaptic vesicles, respectively. βIII-tubulin is shown as a loading control. P1, nuclear & debris; S1, post-nuclear fraction; P2, synaptosomes; S2, crude cytosol; P3, synaptosomal membrane; SC, crude synaptic cytosol; PSD, postsynaptic density; ESM, extrasynaptic membrane.

(E) Brain cell-type-specific expression of eIF4G1. eIF4G1 protein (green) was co-stained with cell-type-specific markers (red) – NeuN (neurons), CaMKIIα (excitatory neurons), GAD67 (inhibitory neurons), GFAP (astrocytes), IBA1 (microglia), or OLIG2 (oligodendrocytes) – in hippocampal CA1 of eIF4G1 wt brain. Nuclei were stained by Hoechst (blue). The white square in the images is enlarged at the right. Scale bar, 20 μm.

Figure S2. eIF4G1 Protein in the eIF4G1-1D Brain

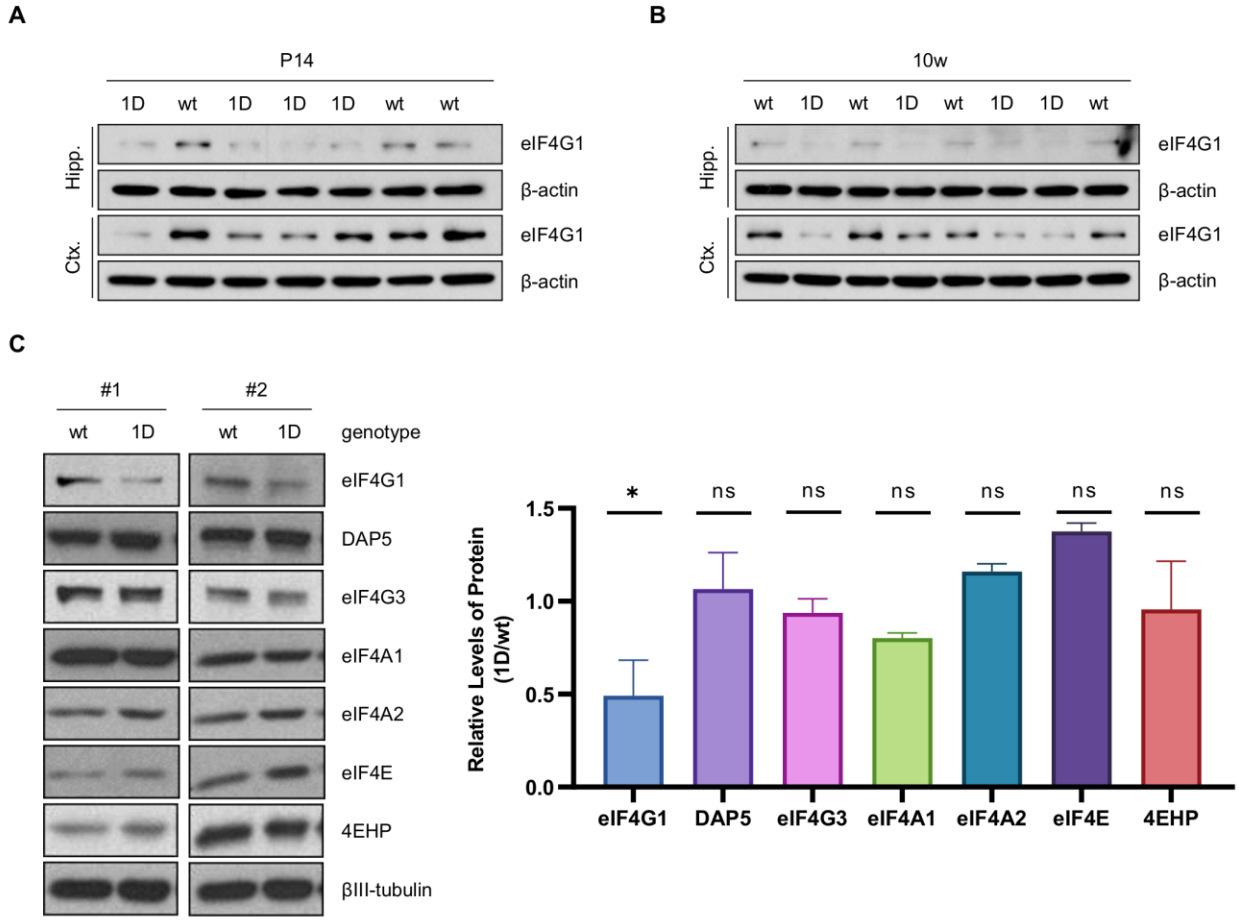

Figure S2. eIF4G1 protein in the eIF4G1-1D brain

(A) eIF4G1 protein levels in the eIF4G1-1D brain on postnatal day 14 (P14). Hippocampus (Hipp.) and cortex (Ctx.) were dissected from the whole mouse brain and subjected to immunoblot analysis. β-actin was used as a loading control.

(B) eIF4G1 protein levels in the 10-week-old (10w) mouse brain. Samples were prepared as described in Panel A.

(C) eIF4F component protein levels in the eIF4G1-1D brain. (Left) Forebrain was dissected from the eIF4G1 wt and 1D mice and subjected to immunoblot analysis. βIII-tubulin was used as a loading control. (Right) Quantification of the ratio of each eIF4F component in eIF4G1-1D to wt brain. The graph is shown as the mean±S.D. of two biological replicates for each genotype; ns, not significant; *$p < 0.05$ (one-way ANOVA followed by Dunnett's post hoc test).

Figure S3. Ribosome Profiling Using P14 Mouse Forebrains

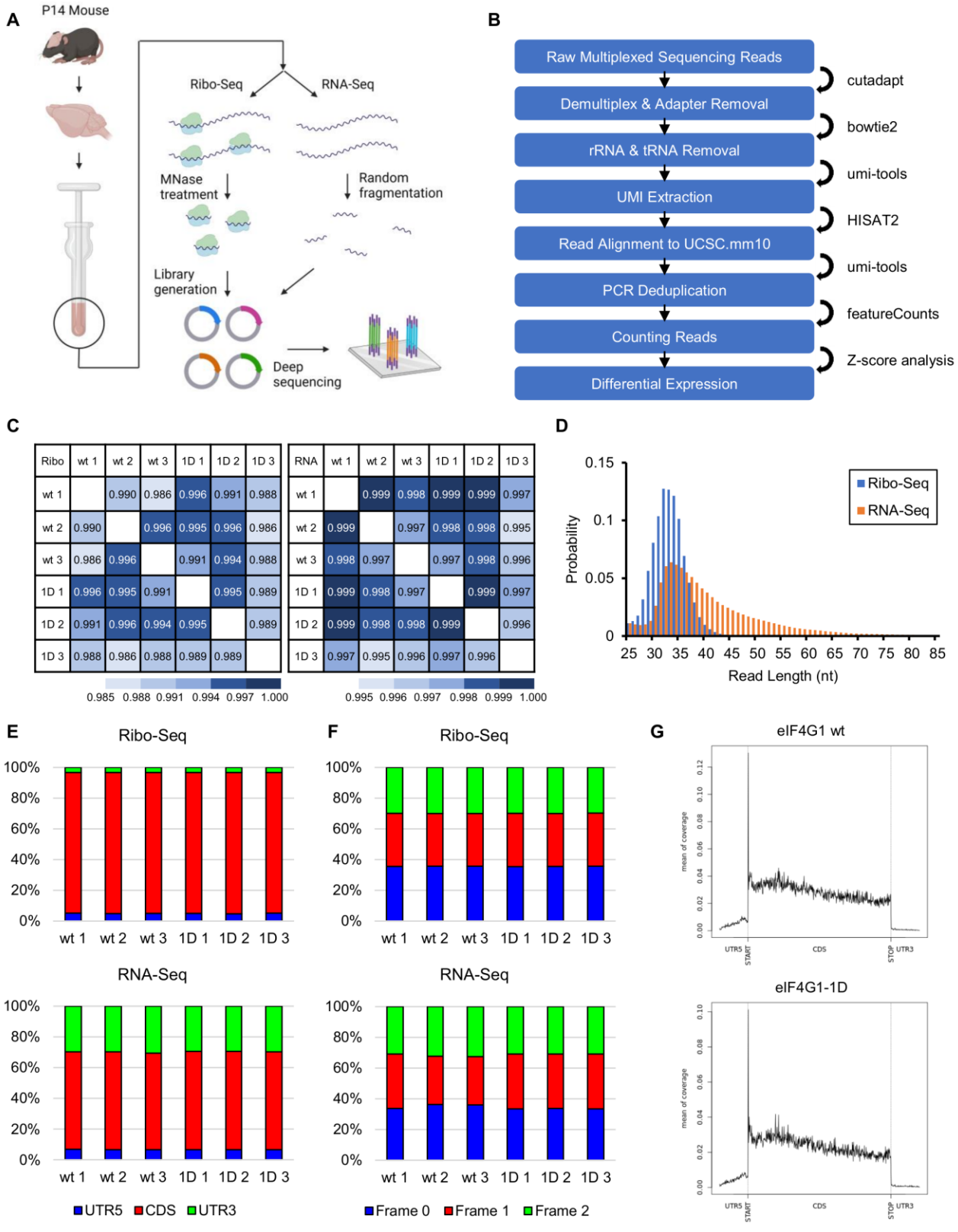

Figure S3. Ribosome profiling using P14 mouse forebrains

(A) Experimental workflow for Ribo-Seq and RNA-Seq library preparation from P14 mouse forebrains.

(B) Ribosome profiling analysis workflow. A list of software used for each step is indicated on the right.

(C) Pearson's correlation coefficient between samples of Ribo-Seq (left) and RNA-Seq (right).

(D) Read length distribution of Ribo-Seq (blue) and RNA-Seq (orange).

(E) Transcript element distribution of Ribo-Seq (upper) and RNA-Seq (lower). 5'-UTR, CDS, and 3'-UTR are indicated as blue, red, and green, respectively.

(F) Reading frame distribution of Ribo-Seq (upper) and RNA-Seq (lower). Percentage of P-site in each frame is shown as blue, red, and green.

(G) Metagene profile of Ribo-Seq from eIF4G1 wt (upper) and eIF4G1-1D (lower) brains.

Figure S4. Axon Outgrowth is Intact in eIF4G1-1D Hippocampal Pyramidal Neurons

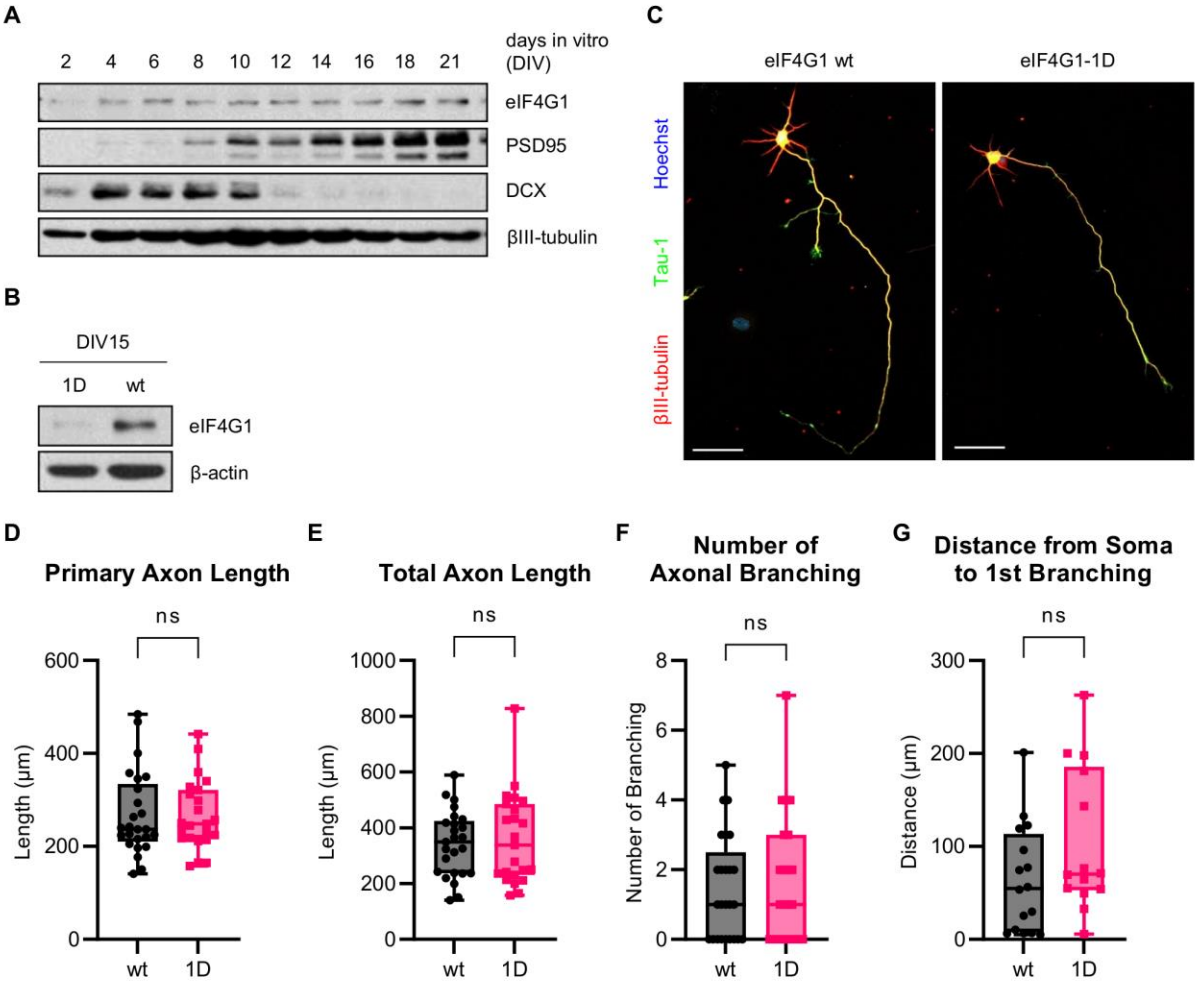

Figure S4. Axon outgrowth is intact in eIF4G1-1D hippocampal pyramidal neurons

(A) eIF4G1 protein levels in developing primary cortical neurons. PSD95 and doublecortin (DCX) were used as control proteins increasing or decreasing during neuronal development, respectively. βIII-tubulin is shown as a loading control.

(B) eIF4G1 protein levels in primary hippocampal neurons at DIV15. β-actin was used as a loading control.

(C) Representative images of DIV3 eIF4G1 wt (left) or eIF4G1-1D (right) hippocampal pyramidal neuron. Axons were stained using Tau-1 (green), and dendrites were stained using βIII-tubulin (red). Nuclei were stained by Hoechst (blue). Scale bar, 50 μm.

(D) Primary axon length. wt (n = 25; 267.720±18.021 μm) vs. 1D (n = 23; 266.462±15.620 μm); ns, not significant; $p = 0.959$ (two-tailed Student's *t*-test).

(E) Total axon length. wt (342.859±23.451 μm) vs. 1D (359.186±34.010 μm); ns, not significant; $p = 0.691$ (two-tailed Student's *t*-test).

(F) Number of axonal branching. wt (1.480±0.301) vs. 1D (1.609±0.386); ns, not significant; $p = 0.792$ (two-tailed Student's *t*-test).

(G) Distance from the soma to the 1st axonal branching. wt (63.948±14.489 μm) vs. 1D (104.591±20.702 μm); ns, not significant; $p = 0.112$ (two-tailed Student's *t*-test).

Figure S5. eIF4G1-1D Mice are Intact in Self-grooming, Locomotor Activity, Anxiety Level, and Motor Learning

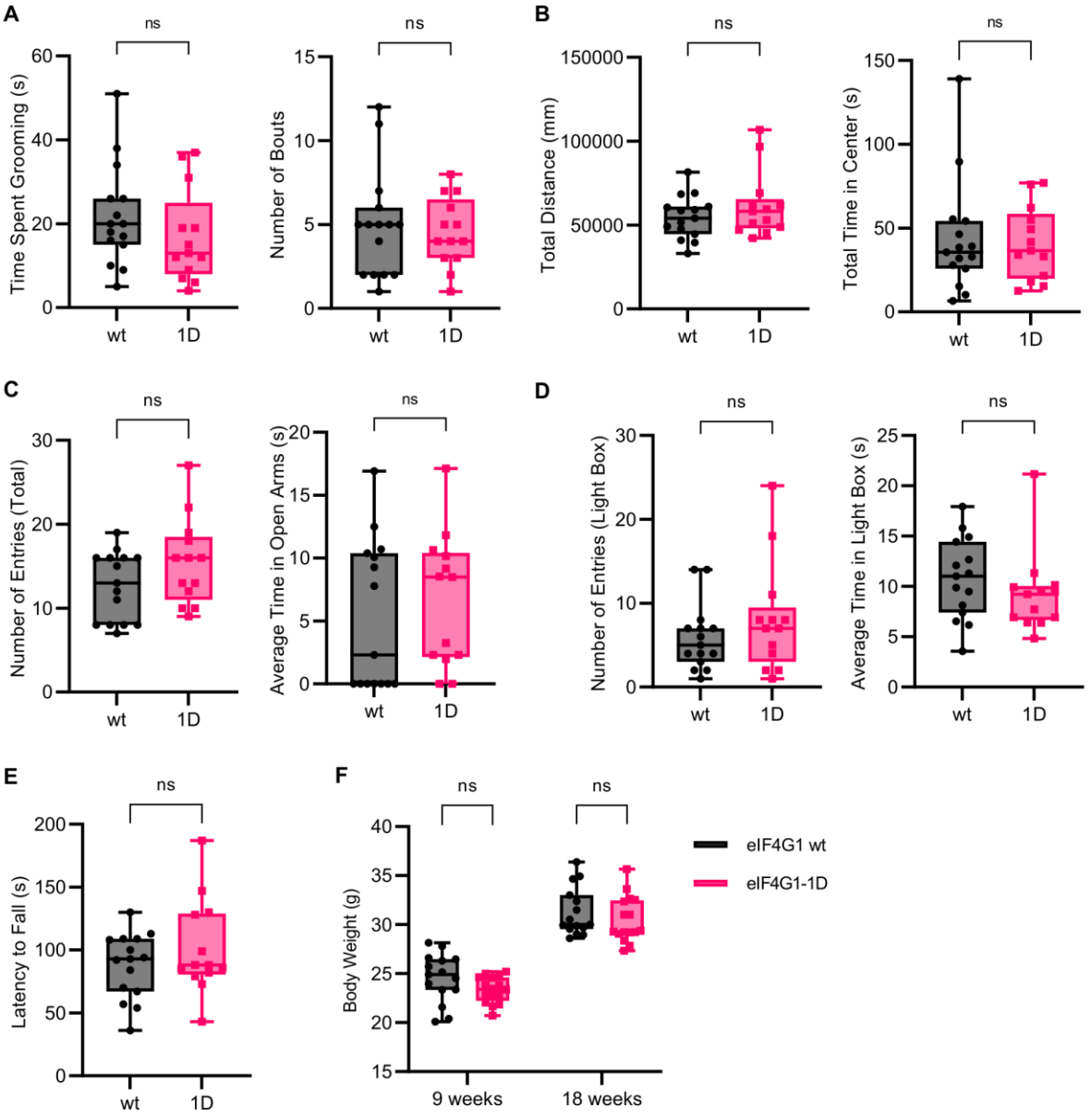

Figure S5. eIF4G1-1D mice are intact in self-grooming, locomotor activity, anxiety level, and motor learning

(A) Self-grooming test. Mice are placed in a new cage equal to the home cage, containing fresh bedding materials without nesting materials, and allowed to explore for 20 min. Self-grooming parameters were measured for 10 min after the habituation phase for the first 10 min. (Left) Total time spent grooming. wt (21.80±3.09 sec) vs. 1D (16.92±3.09 sec); $p = 0.277$. (Right) Total number of grooming bouts. wt (4.93±0.83) vs. 1D (4.54±0.57); ns, not significant; $p = 0.706$.

(B) Open field test. (Left) Total travel distance. wt (54631.86±3324.62 mm) vs. 1D (61650.54±5390.89 mm); $p = 0.264$. (Right) Total time spent in the center. wt (43.22±8.65 sec) vs. 1D (40.96±6.06 sec); ns, not significant; $p = 0.837$.

(C) Elevated plus maze test. (Left) Total number of entries. wt (12.67±1.05) vs. 1D (15.46±1.43); $p = 0.122$. (Right) Average time spent in open arms. wt (5.33±1.53 sec) vs. 1D (6.60±1.47 sec); ns, not significant; $p = 0.557$.

(D) Light-dark transition test. (Left) Number of entries to the light box. wt (5.87±1.01) vs. 1D (8.08±1.81); $p = 0.280$. (Right) Average time spent in the light box. wt (10.76±1.03 sec) vs. 1D (9.23±1.12 sec); ns, not significant; $p = 0.325$.

(E) Rotarod test. Each point represents data from an individual mouse, and values are shown as the mean±S.E.M. n = 15 for eIF4G1 wt and 13 for eIF4G1-1D; wt (87.73±6.72 sec) vs. 1D (101.25±10.40 sec); ns, not significant; $p = 0.277$ (two-tailed Student's *t*-test).

(F) Body weight. wt (n = 15; 24.56±0.64 g) vs. 1D (n = 16; 23.35±0.33 g); $p = 0.242$ (9 weeks); wt (n = 15; 31.27±0.36 g) vs. 1D (n = 16; 30.49±0.58 g); ns, not significant; $p = 0.536$ (18 weeks) (two-way ANOVA followed by Sidak's post hoc test).

Table S1. Comparison of eIF4E and eIF4G1

	eIF4E	eIF4G1
Role in eIF4F	► Cap-binding protein	► Scaffold protein
Translational Control	► Cap-dependent translation	► Cap-dependent translation ► IRES-mediated cap-independent translation (Y. V. Svitkin *et al.*, *Mol Cell Biol*, 2005)
Sensitive Element of mRNA	► Highly structured 5'-UTR (J. Pelletier and N. Sonenberg, *Cell*, 1985)	► Long 3'-UTR ► Multiple upstream open reading frames (uORFs) in 5'-UTR (F. Ramírez-Valle *et al.*, *J Cell Biol*, 2008) ► Translation initiator of short 5'-UTR (TISU) in 5'-UTR (H. Sinvani *et al.*, *Cell Metab*, 2015)
Homozygous Knockout	► Embryonic lethal (P. Sénéchal *et al.*, *Cell Mol Life Sci*, 2021)	► Embryonic lethal (P. Sénéchal *et al.*, *Cell Mol Life Sci*, 2021)
Partial Depletion in Cells	► Non-significant effect on global translation (A. Yanagiya *et al.*, *Mol Cell*, 2012)	► Non-significant effect on global translation (F. Ramírez-Valle *et al.*, *J Cell Biol*, 2008)
Up-regulation	► ASD-like behaviors (eIF4E-transgenic mice) (E. Santini *et al.*, *Nature*, 2013) ► ASD-like behaviors (4E-BP2-knockout mice) (C. G. Gkogkas *et al.*, *Nature*, 2013) ► Spatial memory and motor impairment (4E-BP2 knockout in Purkinje cells) (M. Hooshmandi *et al.*, *Cell Rep*, 2021) ► Susceptible to PTZ-induced seizures (4E-BP2 knockout in PV neurons) (V. Sharma *et al.*, *Proc Natl Acad Sci U S A*, 2021)	► Social deficits and anxiety-like behaviors (CUL3-deficient mice) (Z. Dong *et al.*, *Neuron*, 2020)
Down-regulation	► Long-term memory impairment (eIF4E knockdown in LA excitatory neurons) (P. Shrestha *et al.*, *Nat Neurosci*, 2020) ► Conditioned threat and safety responses disruption (eIF4E knockdown in CeL inhibitory neurons) (P. Shrestha *et al.*, *Nature*, 2020) ► Depression and anxiety-like behaviors (eIF4E S209A knockin mice) (I. S. Amorim *et al.*, *J Neurosci*, 2018; A. Aguilar-Valles *et al.*, *Nat Commun*, 2018)	► Social behavior and memory deficits (Eif4g1 Δμexon mice) (T. Gonatopoulos-Pournatzis *et al.*, *Mol Cell*, 2020)

Dataset S1. Z-score analysis for differentially translated genes in the eIF4G1-1D brain

SI References

1. Y. V. Svitkin, *et al.*, Eukaryotic translation initiation factor 4E availability controls the switch between cap-dependent and internal ribosomal entry site-mediated translation. *Mol Cell Biol* **25**, 10556-10565 (2005).
2. J. Pelletier, N. Sonenberg, Insertion mutagenesis to increase secondary structure within the 5' noncoding region of a eukaryotic mRNA reduces translational efficiency. *Cell* **40**, 515-526 (1985).
3. F. Ramírez-Valle, S. Braunstein, J. Zavadil, S. C. Formenti, R. J. Schneider, eIF4GI links nutrient sensing by mTOR to cell proliferation and inhibition of autophagy. *J Cell Biol* **181**, 293-307 (2008).
4. H. Sinvani, *et al.*, Translational tolerance of mitochondrial genes to metabolic energy stress involves TISU and eIF1-eIF4GI cooperation in start codon selection. *Cell Metab* **21**, 479-492 (2015).
5. P. Sénéchal, *et al.*, Assessing eukaryotic initiation factor 4F subunit essentiality by CRISPR-induced gene ablation in the mouse. *Cell Mol Life Sci* **78**, 6709-6719 (2021).
6. A. Yanagiya, A., *et al.*, Translational homeostasis via the mRNA cap-binding protein, eIF4E. *Mol Cell* **46**, 847-858 (2012).
7. C. A. Hoeffer, *et al.*, Inhibition of the interactions between eukaryotic initiation factors 4E and 4G impairs long-term associative memory consolidation but not reconsolidation. *Proc Natl Acad Sci U S A* **108**, 3383-3388 (2011).
8. P. Shrestha, *et al.*, Cell-type-specific drug-inducible protein synthesis inhibition demonstrates that memory consolidation requires rapid neuronal translation. *Nat Neurosci* **23**, 281-292 (2020).
9. P. Shrestha, *et al.*, Amygdala inhibitory neurons as loci for translation in emotional memories. *Nature* **586**, 407-411 (2020).
10. E. Santini, *et al.*, Exaggerated translation causes synaptic and behavioural aberrations associated with autism. *Nature* **493**, 411-415 (2013).

11. C. G. Gkogkas, *et al.*, Autism-related deficits via dysregulated eIF4E-dependent translational control. *Nature* **493**, 371-377 (2013).

12. M. Hooshmandi, *et al.*, 4E-BP2-dependent translation in cerebellar Purkinje cells controls spatial memory but not autism-like behaviors. *Cell Rep* **35**, 109036 (2021).

13. V. Sharma, *et al.*, 4E-BP2-dependent translation in parvalbumin neurons controls epileptic seizure threshold. *Proc Natl Acad Sci U S A* **118**, e2025522118 (2021).

14. I. S. Amorim, *et al.*, Loss of eIF4E Phosphorylation Engenders Depression-like Behaviors via Selective mRNA Translation. *J Neurosci* **38**, 2118-2133 (2018).

15. A. Aguilar-Valles, *et al.*, Translational control of depression-like behavior via phosphorylation of eukaryotic translation initiation factor 4E. *Nat Commun* **9**, 2459 (2018).

16. Z. Dong, *et al.*, CUL3 deficiency causes social deficits and anxiety-like behaviors by impairing excitation-inhibition balance through the promotion of cap-dependent translation. *Neuron* **105**, 475-490.e6 (2020).

17. T. Gonatopoulos-Pournatzis, *et al.*, Autism-misregulated eIF4G microexons control synaptic translation and higher order cognitive functions. *Mol Cell* **77**, 1176-1192.e16 (2020).

18. J. Li, *et al.*, Synaptic P-Rex1 signaling regulates hippocampal long-term depression and autism-like social behavior. *Proc Natl Acad Sci U S A* **112**, E6964-E6972 (2015).

19. S.-H. Kim, *et al.*, Mitochondrial threonyl-tRNA synthetase TARS2 is required for threonine-sensitive mTORC1 activation. *Mol Cell* **81**, 398-407.e4 (2021).

20. N. J. McGlincy, N. T. Ingolia, Transcriptome-wide measurement of translation by ribosome profiling. *Methods* **126**, 112-129 (2017).

21. J. Steinberger, *et al.*, Identification and characterization of hippuristanol-resistant mutants reveals eIF4A1 dependencies within mRNA 5′ leader regions. *Nucleic Acids Res* **48**, 9521-9537 (2020).

22. M. Martin, Cutadapt removes adapter sequences from high-throughput sequencing reads. *EMBnet.journal* **17**, 10-12 (2011).

23. B. Langmead, S. L. Salzberg, Fast gapped-read alignment with Bowtie 2. *Nat Methods* **9**, 357-359 (2012).

24. T. Smith, A. Heger, I. Sudbery, UMI-tools: modeling sequencing errors in unique molecular identifiers to improve quantification accuracy. *Genome Res* **27**, 491-499 (2017).

25. D. Kim, J. M. Paggi, C. Park, C. Bennett, S. L. Salzberg, Graph-based genome alignment and genotyping with HISAT2 and HISAT-genotype. *Nat Biotechnol* **37**, 907-915 (2019).

26. Y. Liao, G. K. Smyth, W. Shi, featureCounts: an efficient general purpose program for assigning sequence reads to genomic features. *Bioinformatics* **30**, 923-930 (2014).

27. S. J. Kiniry, P. B. F. O'Connor, A. M. Michel, P. V. Baranov, Trips-Viz: a transcriptome browser for exploring Ribo-Seq data. *Nucleic Acids Res* **47**, D847-D852 (2019).

28. J. Ou, M. Hoye, ribosomeProfilingQC: Ribosome Profiling Quality Control. R package version 1.8.0. 10.18129/B9.bioc.ribosomeProfilingQC (2022).

29. R. Yousefi, *et al.*, Monitoring mitochondrial translation in living cells. *EMBO Rep* **22**, e51635 (2021).

30. M. Zorkau, C. A. Albus, R. Berlinguer-Palmini, Z. M. A. Chrzanowska-Lightowlers, R. N. Lightowlers, High-resolution imaging reveals compartmentalization of mitochondrial protein synthesis in cultured human cells. *Proc Natl Acad Sci U S A* **118**, e2008778118 (2021).

31. S. Arai, *et al.*, RGB-color intensiometric indicators to visualize spatiotemporal dynamics of ATP in single cells. *Angew Chem Int Ed Engl* **57**, 10873-10878 (2018).

32. C. V. Vorhees, M. T. Williams, Morris water maze: procedures for assessing spatial and related forms of learning and memory. *Nat Protoc* **1**, 848-858 (2006).